Carrier type dependence on spatial asymmetry of unipolar resistive switching of metal oxides

Kazuki Nagashima, Takeshi Yanagida, Masaki Kanai, Umberto Celano, Sakon Rahong et al.

Citation: Appl. Phys. Lett. **103**, 173506 (2013); doi: 10.1063/1.4826558
View online: http://dx.doi.org/10.1063/1.4826558
View Table of Contents: http://apl.aip.org/resource/1/APPLAB/v103/i17
Published by the AIP Publishing LLC.

Carrier type dependence on spatial asymmetry of unipolar resistive switching of metal oxides

Kazuki Nagashima,[1] Takeshi Yanagida,[1,a)] Masaki Kanai,[1] Umberto Celano,[2] Sakon Rahong,[1] Gang Meng,[1] Fuwei Zhuge,[1] Yong He,[1] Bae Ho Park,[3] and Tomoji Kawai[1,3]

[1]*The Institute of Scientific and Industrial Research, Osaka University, 8-1 Mihogaoka Ibaraki, Osaka 567-0047, Japan*

[2]*K. U. Leuven at IMEC, Kapeldreef 75, B-3001 Leuven, Belgium*

[3]*Division of Quantum Phases & Devices, Department of Physics, Konkuk University, Seoul 143-701, South Korea*

(Received 26 August 2013; accepted 9 October 2013; published online 22 October 2013)

We report a carrier type dependence on the spatial asymmetry of unipolar resistive switching for various metal oxides, including NiO_x, CoO_x, TiO_{2-x}, YSZ, and SnO_{2-x}. *n*-type oxides show a unipolar resistive switching at the anode side whereas *p*-type oxides switch at the cathode side. During the forming process, the electrical conduction path of *p*-type oxides extends from the anode to cathode while that of *n*-type oxides forms from the cathode to anode. The carrier type of switching oxide layer critically determines the spatial inhomogeneity of unipolar resistive switching during the forming process possibly triggered via the oxygen ion drift. © *2013 AIP Publishing LLC*. [http://dx.doi.org/10.1063/1.4826558]

A resistive switching in metal/oxide/metal junctions has proven potential for next-generation nonvolatile memories due to the structural simplicity and also the memory characteristics superior to existing other memories.[1–3] Although intensive efforts have been devoted to elucidate the intrinsic origin of the resistive switching, the knowledge as to the exact switching mechanisms is still required.[4–9] One reason why it has been difficult to fully understand the nature of resistive switching is that the resistive switching event intrinsically involves the spatially inhomogeneous physical phenomena.[10,11] Previous studies have highlighted that such spatial inhomogeneity is mainly induced by the so-called "forming process," which is defined as an initial process to introduce an electrical conduction path within pristine insulative samples by applying the relatively high electric field.[11,12] The forming process affects not only the degree of spatial inhomogeneity on the electrical conduction within resistive devices but also the nonvolatile memory characteristics.[11,12] Although the nature of forming process has been interpreted in terms of a soft dielectric breakdown phenomenon,[11] understanding the exact mechanisms of forming process is still not comprehensive due to the inherent complexity of dielectric breakdown phenomenon within solids.[13,14] Use of device structures with multi-electrodes is one of the ways to detect the spatial information of forming process.[15–17] For example, Kim *et al*. have reported the inhomogeneity of electrical conditions of unipolar resistive switching in three terminal devices comprised NiO.[16] In most cases, the inhomogeneity of electrical conductions for unipolar switching is induced by the forming process.[15–17] By considering the dielectric breakdown nature of the forming process, one can expect that the material properties of switching layers, including the carrier type, affect the inhomogeneity of electrical conduction during the forming process although such knowledge is still scarce. Here we demonstrate the carrier type dependence on the spatial inhomogeneity of unipolar resistive switching by utilizing three terminal devices comprised various metal oxides.

NiO_x, CoO_x, TiO_{2-x}, ytteria stabilized zirconia (YSZ), and SnO_{2-x} thin films were grown on Pt/TiO_{2-x}/Si (100) substrate by pulsed laser deposition (PLD) method (ArF excimer, $\lambda = 193$ nm). The film thickness was controlled to be 50 nm. Prior to the deposition of thin films, the Pt bottom electrode was deposited onto the substrate with TiO_{2-x} adhesion layer. The reason why TiO_{2-x} was utilized as adhesion layer instead of conventionally used Ti is to prevent the thermal diffusion of Ti into the switching layer during the switching process, which crucially affects the resistive switching.[18] The thickness of Pt bottom electrode was 100 nm. Oxygen pressures were optimized to be 10 Pa for TiO_{2-x}, YSZ, SnO_{2-x}, and 10^{-3} Pa for CoO_x and 10^{-1} Pa for NiO_x during the deposition of thin films. Substrate temperature of 300 °C was used for NiO_x and 500 °C for CoO_x, TiO_{2-x}, YSZ, and room temperature for SnO_{2-x}, respectively. The oxide target was used, which was obtained by sintering the milled powder (99.99% pure) at 1000 °C for 24 h. The laser power, the repetition rate, and the distance between the target and the substrate were set to be 40 mJ, 10 Hz, and 30 mm, respectively. The Pt top electrode was then deposited onto the thin films by using a metal mask of $25 \times 25\ \mu m^2$. Note that Pt was utilized as electrodes to avoid the effect of oxidization of metal electrode. X-ray diffraction (XRD) was used to evaluate the crystal structure of the fabricated films. Current-voltage (I-V) characteristics were evaluated using semiconductor parameter analyzer (Keithley 4200-SCS) at room temperature in the ambient atmosphere.

Fig. 1 shows the schematic of three terminal devices employed in this study. First, we perform the forming process between electrode A and electrode C by applying a relatively high electric field around 10 V range. Note that the electrode B is floating during the forming process. The

a)Corresponding author. yanagi32@sanken.osaka-u.ac.jp

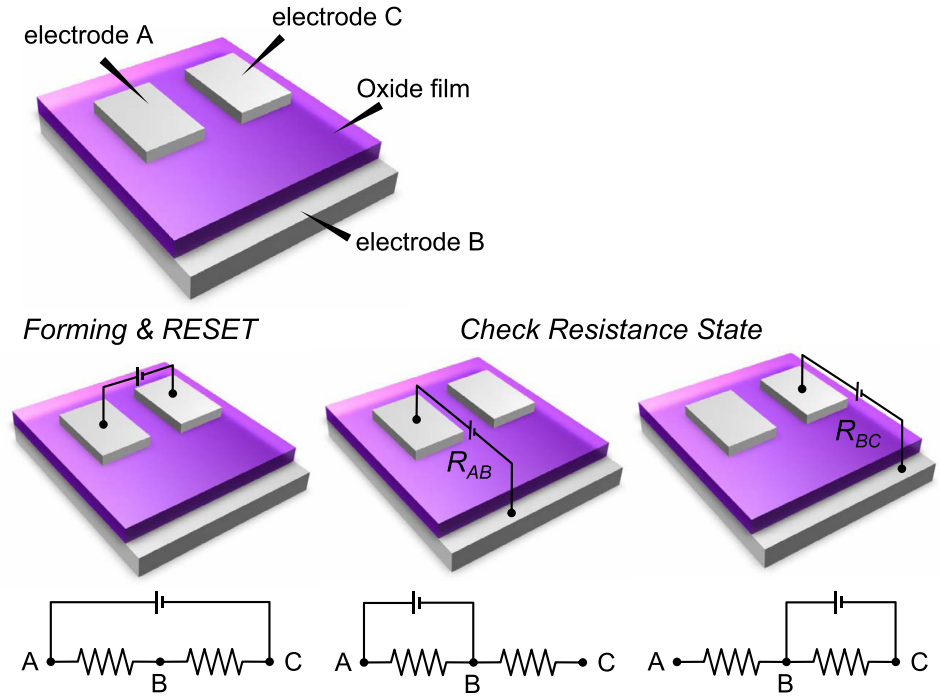

FIG. 1. Schematic of three terminal devices employed.

compliance current is set to be 10 mA, which is defined as an upper limited current value when increasing an electric field for the forming process. After the forming process, the resistance state changes from insulative pristine state to conductive ON state. ON state is defined as a state that the current can highly flow. Then we perform the RESET process to obtain insulative OFF state between A-C electrodes by applying the electric field around a few V. OFF state is defined as a state that the current flow is lower. In these forming and RESET processes, we set the electrode A as the anode and the electrode C as the cathode. After the RESET process, we measure the I-V data of between A-B electrodes and between B-C electrodes. Fig. 2 shows the I-V data for various metal oxides, including NiO_x, CoO_x, YSZ, TiO_{2-x}, and SnO_{2-x}. The trends of measured I-V data can be classified into two groups. One group shows that the resistance between A-B electrodes (R_{AB}) is much higher than that between B-C electrodes (R_{BC}), indicating that the switching mainly occurs at the anode side. This trend is commonly observed for TiO_{2-x}, YSZ, and SnO_{2-x}, which are known as *n*-type oxides in bulk.[19] In contrast, the other group shows that R_{BC} is much higher than R_{AB}, indicating that the switching mainly occurred at the cathode side. This complete opposite trend is found for NiO, and CoO_x, which are known as *p*-type oxides in bulk.[20,21] To more clearly show the difference between the two groups, we obtain the resistance ratio data of R_{AB} to R_{BC} after the forming and RESET processes in A-C electrodes as shown in Fig. 3. For *n*-type oxides including YSZ, TiO_{2-x}, and SnO_{2-x}, R_{AB} at the anode side is always higher than R_{BC} at the cathode side for both high

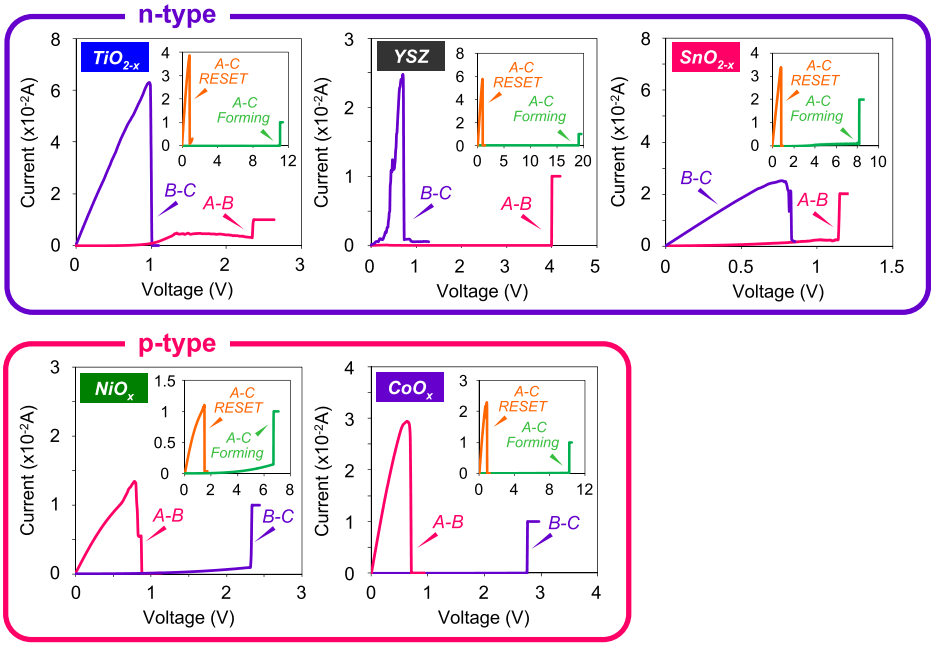

FIG. 2. Typical I-V data of AB and BC electrode configurations after RESET process in AC electrode configuration. Insets show the initial forming and RESET processes of AC electrode configuration.

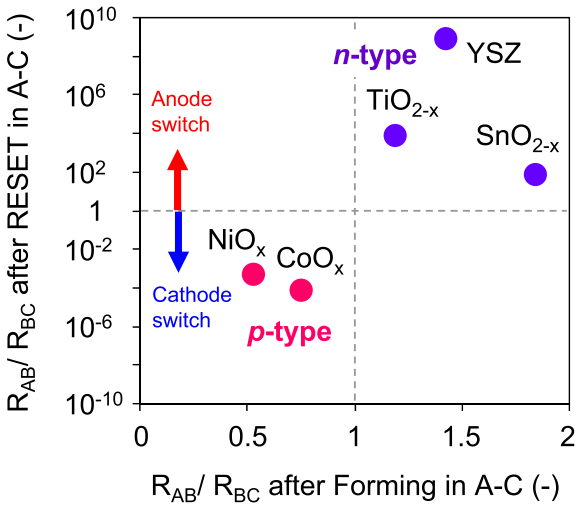

FIG. 3. Comparison of resistance change between AB and BC electrode configurations for various metal oxides.

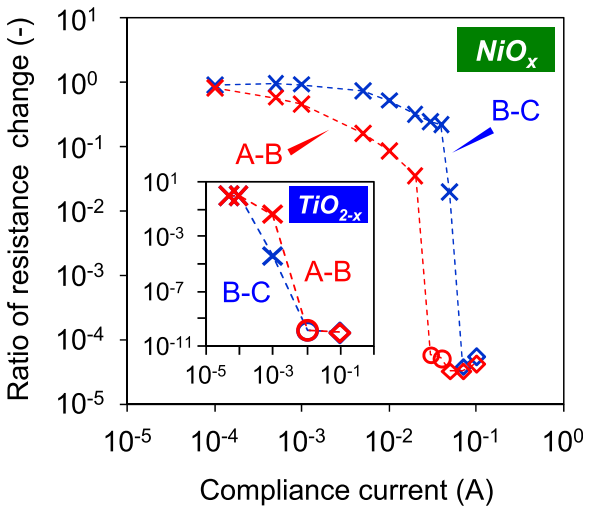

FIG. 4. Change in resistance data (R_{AB} and R_{BC}) of AB and BC electrode configurations when varying the compliance current for forming process in the case of NiO_x. Inset for TiO_{2-x}. The symbols represent the incomplete forming process (×), the complete forming process (○), and permanent electric breakdown (◇), respectively.

resistance state and low resistance state conditions. On the other hand, for *p*-type oxides including NiO_x and CoO_x, R_{BC} at the cathode side is higher than R_{AB} at the anode side. Thus, there is a clear difference between *n*-type oxides and *p*-type oxides on the spatial asymmetry of unipolar resistive switching.

Here we discuss what essentially causes above spatial discrepancy between *n*-type and *p*-type oxides on the resistive switching trends. Since the resistive switching occurring at the higher resistive portion during the RESET process is rational by taking into account the Joule heating model, the spatial asymmetry of resistive switching between *n*-type and *p*-type oxides should emerge during the forming process. First, we examine how the forming process creates the spatial asymmetry as seen in the resistance values of R_{AB} and R_{BC}. To observe such evolution of spatial difference during forming process, we vary the compliance current ranged from 10^{-4} to 10^{-1}A. This compliance current variation should control the spatial extension of electrical conduction path during the forming process. Fig. 4 shows the change in resistance data of R_{AB} and R_{BC} when varying the compliance current for forming process between A-C electrodes. The data for NiO_x and TiO_{2-x} are shown in the figure. For TiO_{2-x}, when increasing the compliance current, R_{BC} value first decreases and then further increasing the compliance current results in the decrease of R_{AB}. In contrast, for NiO_x, R_{AB} first decreases when increasing the compliance current, and then further increasing the compliance current results in the decrease of R_{BC}. These experimental data highlight that the spatial asymmetry of electrical conduction emerges during the forming process, and the spatial trend in the forming process of *n*-type oxides is in sharp contrast to that of *p*-type oxides.

Two models have been proposed to interpret experimental trends of three terminal devices, including (i) one anode-one cathode model and (ii) two anodes-two cathodes model.[16] Our electric field simulations demonstrate that (ii) two anodes-two cathodes model is appropriate for our device geometry, as shown in Fig. 5(a). However, the two anodes-two cathodes model cannot explain our experimental results as to spatial asymmetry because of the same electric field spatial distributions for both the gap between A and B electrodes and the gap between B and C electrodes. One of the possible scenarios to explain our experimental trends even within the framework of two anodes-two cathodes model is to consider the difference between the interface with top electrode and the interface with bottom electrode. If such asymmetry in the two interfaces exists in our devices, the electric field is no longer symmetric when the polarity of electric field is inversed. To validate above scenario based on the interface asymmetry, we have examined the effect of polarity inversion on the forming processes of two terminal devices by varying the compliance currents. Fig. 5(b) shows

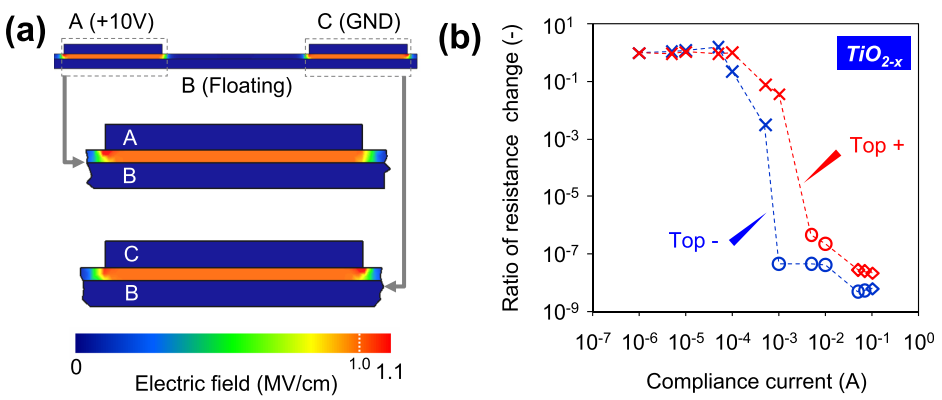

FIG. 5. (a) Electric field simulation for our three terminal device structure. (b) Effect of polarity inversion on the change in the resistance data of AB electrode configurations with varying the compliance current. The symbols represent the incomplete forming process (×), the complete forming process (○), and permanent electric breakdown (◇), respectively.

the effect of polarity inversion on the resistance change data of R_{AB} when varying the compliance current during the forming. The data of TiO_{2-x} are shown in the figure. The forming process for the negatively biased top electrode emerges at the compliance currents lower than that for the positively biased top electrode. Since it is well known that the forming process induces the electrical conduction from the cathode to the anode for *n*-type oxides, the results in Fig. 5(b) indicate that the forming process can be more readily triggered from the top electrode rather than the bottom electrode in the present devices. Although it is difficult to identify what exactly differs from between the two interfaces at the moment, various factors, including interface roughness and interfacial defects might be responsible. This polarity inversion dependence on the forming process can explain the difference between A-B electrodes and B-C electrodes in Fig. 4 in terms of the difference between the two interfaces. As seen in Fig. 5(b), the forming process from the top interface starts to occur at the electric fields lower than that required for the bottom interface. Thus, for *n*-type oxides, the forming process first occurs from the top C electrode (cathode) to the bottom B electrode (anode) rather than from the bottom B electrode (cathode) to the top A electrode (anode). The same scenario can explain the inversed situation for *p*-type oxides. However, it should be emphasized that the scenario based on only the effect of two interface difference on the forming process alone cannot explain the significant difference between *n*-type oxides and *p*-type oxides on the results of Figs. 2–4. This is because the two interface difference cannot show the opposite trend between *n*-type and *p*-type oxides in the resistance data of R_{AB} and R_{BC} during the forming process. Thus, the effect of carrier type on the spatial asymmetry during the forming process is an intrinsic feature rather than an artifact due to specific device configurations.

Finally we discuss what possibly causes the dependence of carrier type on the forming process although we have no direct experimental evidences to address this issue at the moment. The polarity dependence of charged ion motion might be related to our experimental observations. From previous works as to resistive switching,[22] it is reasonable to assume the occurrence of oxygen ion drift during the forming process. The issue is how we can interpret the carrier type dependence on the spatial asymmetry of forming process in terms of the oxygen ion drift. The oxygen ion drift gradually results in the spatial inhomogeneity of conductivity within the switching layer during the forming process.[23] According to our previous model based on dual defects (oxygen and cation vacancies), for *n*-type oxides, the oxygen ionic drift can create the electrical conduction from near the cathode side via increasing the concentration of oxygen vacancies near the cathode since negatively charged oxygen ions are depleted from the cathode when applying the electric field. In contrast, the oxygen ionic drift creates the electrical conduction from the anode side for *p*-type oxides via increasing the concentration of apparent cation vacancies near the anode.[24] The ionic drift induced conductive spatial portion seems to trigger the forming process and the portion may form from near the top electrode as discussed above, resulting in $R_{AB}/R_{BC} > 1$ for *n*-type oxides and $R_{AB}/R_{BC} < 1$ for *p*-type oxides after the forming process as seen in Fig. 3. Thus the carrier type dependence on the spatial asymmetry of resistive switching can be interpreted in terms of the oxygen ionic drift. Although the carrier type dependence on the switching location of bipolar resistive switching has been reported,[25,26] our results highlight that the ionic drift events might trigger the forming process and determine the switching location of unipolar resistive switching.

We demonstrated the carrier type dependence on the spatial asymmetry of unipolar resistive switching by utilizing three terminal devices comprised Pt electrodes and various polycrystalline metal oxide layers, including CoO_x, NiO_x, TiO_{2-x}, YSZ, and SnO_{2-x}. After the forming process between the two top electrodes interposed via the middle bottom electrode, *n*-type oxides showed the unipolar resistive switching at the anode side, whereas *p*-type oxides switched at the cathode side. During the forming process, the electrical conduction of *p*-type oxides extended from the anode to cathode, while that of *n*-type oxides formed from the cathode to anode. Thus the carrier type of switching oxide layer critically determines the spatial asymmetry of unipolar resistive switching during the forming process possibly triggered via the oxygen ion drift.

This study was supported by NEXT. T.K. was supported by FIRST program. B.H.P. was supported by the NRF grant funded by the Korea government (MSIP) (No. 2013R1A3A2042120). K.N. was supported by Grant-in-Aid for Challenging Exploratory Research (No. 24651138).

[1]R. Waser and M. Aono, Nature Mater. **6**, 833 (2007).
[2]M.-J. Lee, C. B. Lee, D. Lee, S. R. Lee, M. Chang, J. H. Hur, Y.-B. Kim, C.-J. Kim, D. H. Seo, S. Seo, U.-I. Chung, I.-K. Yoo, and K. Kim, Nature Mater. **10**, 625 (2011).
[3]K. Nagashima, T. Yanagida, K. Oka, M. Taniguchi, T. Kawai, J.-S. Kim, and B. H. Park, Nano Lett. **10**, 1359 (2010).
[4]R. Waser, R. Dittmann, G. Staikov, and K. Szot, Adv. Mater. **21**, 2632 (2009).
[5]D.-H. Kwon, K. M. Kim, J. H. Jang, J. M. Jeon, M. H. Lee, G. H. Kim, X.-S. Li, G.-S. Park, B. Lee, S. Han, M. Kim, and C. S. Hwang, Nat. Nanotechnol. **5**, 148 (2010).
[6]J. J. Yang, D. B. Strukov, and D. R. Stewart, Nat. Nanotechnol. **8**, 13 (2013).
[7]K. Oka, T. Yanagida, K. Nagashima, T. Kawai, J.-S. Kim, and B. H. Park, J. Am. Chem. Soc. **132**, 6634 (2010).
[8]K. Nagashima, T. Yanagida, M. Kanai, K. Oka, A. Klamchuen, S. Rahong, G. Meng, M. Horprathum, B. Xu, F. W. Zhuge, Y. He, and T. Kawai, Jpn. J. Appl. Phys., Part 1 **51**, 11PE09 (2012).
[9]K. Nagashima, T. Yanagida, K. Oka, M. Kanai, A. Klamchuen, S. Rahong, G. Meng, M. Horprathum, B. Xu, F. W. Zhuge, Y. He, B. H. Park, and T. Kawai, Nano Lett. **12**, 5684 (2012).
[10]B. J. Choi, D. S. Jeong, S. K. Kim, C. Rohde, S. Choi, J. H. Oh, H. J. Kim, C. S. Hwang, K. Szot, R. Waser, B. Reichenberg, and S. Tiedke, J. Appl. Phys. **98**, 033715 (2005).
[11]T. Yanagida, K. Nagashima, K. Oka, M. Kanai, A. Klamchuen, B. H. Park, and T. Kawai, Sci. Rep. **3**, 1657 (2013).
[12]J. S. Lee, S. B. Lee, S. H. Chang, L. G. Gao, B. S. Kang, M.-J. Lee, C. J. Kim, T. W. Noh, and B. Kahng, Phys. Rev. Lett. **105**, 205701 (2010).
[13]J. J. O' Dwyer, J. Electrochem. Soc. **116**, 239 (1969).
[14]S. Lombardo, J. H. Stathis, B. P. Linder, K. L. Pey, F. Palumbo, and C. H. Tung, J. Appl. Phys. **98**, 121301 (2005).
[15]K. M. Kim, B. J. Choi, Y. C. Shin, S. Choi, and C. S. Hwang, Appl. Phys. Lett. **91**, 012907 (2007).
[16]K. M. Kim, B. J. Choi, S. J. Song, G. H. Kim, and C. S. Hwang, J. Electrochem. Soc. **156**, G213 (2009).
[17]K. Nagashima, T. Yanagida, K. Oka, and T. Kawai, Appl. Phys. Lett. **94**, 242902 (2009).

[18]J. J. Yang, J. P. Strachan, Q. Xia, D. A. A. Ohlberg, P. J. Kuekes, R. D. Kelley, W. F. Stickle, D. R. Stewart, G. Medeiros-Ribeiro, and R. S. Williams, Adv. Mater. **22**, 4034 (2010).
[19]M. M. Arafat, B. Dinan, S. A. Akbar, and A. S. M. A. Haseeb, Sensors **12**, 7207 (2012).
[20]M.-K. Lee and Y.-T. Lai, J. Phys. D: Appl. Phys. **46**, 055109 (2013).
[21]Y.-Q. Mao, Z.-J. Zhou, T. Ling, and X.-W. Du, RSC Adv. **3**, 1217 (2013).
[22]D. B. Strukov and R. S. Williams, Appl. Phys. A **94**, 515 (2009).
[23]K. M. Kim, B. J. Choi, and C. S. Hwang, Appl. Phys. Lett. **90**, 242906 (2007).
[24]K. Oka, T. Yanagida, K. Nagashima, M. Kanai, B. Xu, B. H. Park, H. Katayama-Yoshida, and T. Kawai, J. Am. Chem. Soc. **134**, 2535 (2012).
[25]K. Oka, T. Yanagida, K. Nagashima, M. Kanai, T. Kawai, J.-S. Kim, and B. H. Park, J. Am. Chem. Soc. **133**, 12482 (2011).
[26]K. Nagashima, T. Yanagida, K. Oka, M. Kanai, A. Klamchuen, J.-S. Kim, B. H. Park, and T. Kawai, Nano Lett. **11**, 2114 (2011).